Functional tunability of biological circuits from tinkers

Changhong Shi

School of Mathematics and Computational Sciences and Guangdong Province Key Laboratory of Computational Science, Sun Yat-Sen University,

Guangzhou, P.R. China

Tianshou Zhou

School of Mathematics and Computational Sciences and Guangdong Province Key Laboratory of Computational Science, Sun Yat-Sen University,

Guangzhou, P.R. China

Abstract—In many complex regulatory networks with interlinked feedback loops, the simple core circuits are sufficient to achieve specific biological functions of the entire networks, naturally raising a question: what is the role of the additional feedback loops. Here, by investigating auto-activation and activator-repressor circuits, two most common functional motifs in regulatory networks, we show that the toggle switch acts as a tinker to elaborate the dynamical behavior of both circuits. Specifically, the additional loop does not significantly affect the stable states of the auto-activation circuit but can tune the stimulation threshold for switch (i.e., the minimal stimulus required to switch the system from the low to the high state). For the activator- repressor circuit, the tinker can tune the stimulation threshold for oscillation (i.e., the bifurcation point to generate oscillations) as well as the oscillation frequency but does not change the oscillation amplitude. These detailed results not only provide guidelines to the engineering of both synthetic circuits but also imply a significant fact that additional loops of the core circuit in a complex network are not really redundant but play a role of tuning the network's function

Keywords- Network motif, tunability, biological function, tinker, feedback loop

I. INTRODUCTION

In general, regulatory networks in signaling systems are very complex, possibly involving the regulations of thousands of species molecules and the interactions between them. In spite of this complexity, the regulatory networks are composed of several simple circuits, some of which carry out biological functions similar to those of the entire networks, thus being essential (called as the core circuits)[1-4], and the others act as tinkers for the core circuits to achieve more elaborate functions[5-10], thus being secondary (called as additional circuits or tinkers). Most of previous studies focused on the functions of simple circuits such as auto-activation circuit, feed forward loop, double feedback loops (e.g., toggle switch) and activator-repressor circuit[4], but it seems to us that few addressed the issues such as why circuits or loops additional to the core circuits are necessary and what detailed roles they play in the underlying whole networks. Quantitatively analyzing the role of diverse tinkers in regulatory networks is fundamentally important for understanding the structure and function of more complex networks as well as design principles in synthetic biology.

Core circuits and the related tinkers have been identified in many regulatory networks. For example, in *Bacillus Subtilis* [11-13], as the master regulator, ComK regulates its expression, forming a positive feedback circuit. This circuit is a core module in the *B. Subtilis* system since it can generate a bistable expression pattern essential to competence development [11]. However, besides the ComK protein, the RoK protein binds directly to the comK promoter and acts negatively, and in turn, it is also negatively regulated by ComK, thus creating a double negative feedback loop (i.e., the common toggle switch) [12]. Previous experimental results have shown that when RoK is inactivated, more than half of the cells become competent and the transformation frequency increases correspondingly [14]. Another example is a common regulatory network related to the process of embryonic cell cycle. The circuit responsible for the cell cycle is a negative feedback loop, which is comprised of the cyclin-dependent protein kinase CDK1 and the anaphase-promoting complex (APC) [15, 16]. This feedback loop is sufficient to generate oscillations, implying that it is the core circuit of the entire network. However, the cyclin-CDK1 network also includes two additional positive feedback loops: Active Cdc25 activates CDK1, which further activates Cdc25, forming a double positive feedback loop; Active Wee1 inactivates CDK1, which in turn inactivates Wee1, forming a double negative feedback loop.

The above two examples as well as those listed in the following Table 1 have a common topology, that is, one or two toggle switches are added to the core circuits, e.g., in the first example, the common toggle switch is added to an auto-regulatory circuit whereas in the second example, two kinds of toggle switches (i.e., the common toggle switch and an alternative circuit) are added to a negative feedback circuit. Although the single toggle switch as a basic circuit has been extensively investigated [17] and has also been successfully constructed in *Escherichia coli* [18], and although recent numerical evidences have shown that a simple positive feedback loop can allow a three-component negative feedback oscillatory system to achieve a widely tunable period and a near-constant amplitude [10], it remains to be fully explored how the toggle switch as a secondary module

Table 1 Toggle switch appearing as a secondary module in some regulatory systems.

systems	reactions	reference
EGF receptor signaling	sheddases → EGFR → sheddases PTP ⊣ EGFR ⊣ PTP	[19]
Start of cell cycle in budding yeast	Cln → cdc28 → Cln Sic1 ⊣ cdc28 ⊣ Sic1	[12]
Th1 and Th2 differentiation	STAT6 → GATA3 → STAT6 STAT4 ⊣ GATA3 ⊣ STAT4	[20]
B.subtilis competence events	ComS ⊣ ComK → ComS RoK ⊣ ComK ⊣ RoK	[14, 12]
Mitotic trigger in Xenopus	Cdc25 ⊣ cdc2 → Cdc25 Myt ⊣ cdc2 ⊣ Myt	[16]

of more complex networks affects dynamics of the core circuits.

Bistability (by which we mean that the system of interest has two distinct stable states) and oscillation are two lasting topics in the study of dynamical systems. They are two fundamentally different kinds of dynamical behaviors in the deterministic sense, but can be viewed as the basically similar behavior in the stochastic sense since periodic oscillations are essentially a kind of switching between valleys and peaks [21, 22]. A simple example that can help understand this point is that relaxation-type oscillations arise from a bistable switch [23, 10]. Intuitively, the toggle switch might play a similar role when it is added to a bistable or oscillatory system. In this paper, we will show detailed roles of the toggle switch in tuning functions of two common circuits potential to generate bistability and oscillation, and in particular reveal the mechanism of the tunable roles.

We add the common toggle switch to two prototypical genetic circuits (referring to Fig. 1): the auto-activation circuit (called as Circuit Ⅰ) and the two-component activator-repressor circuit (called as Circuit Ⅱ). These two circuit topologies are common in genetic switch systems and cellular oscillators, such as cell cycle[15, 24], circadian clocks [25] and competence development [12, 26], so elucidating the role of the additional toggle switch in the shared topologies will be of general significance for understanding fundamental intracellular processes. In addition, understanding the mechanisms of how the additional toggle switch affects these simple circuits could guide the engineering of synthetic circuits with detailed nonlinear dynamical behaviors.

To investigate the role of the toggle switch in the bistable and oscillatory systems, we use the method of theory analysis aided by numerical simulation. The bistable system has a well defined stimulation threshold for response to environmental stimulation, and only stimulation above the threshold can switch the system from the low to the high state in the state space. The numerical and theoretical analysis shows that the additional toggle switch can enhance the stimulation threshold significantly but has little influence on
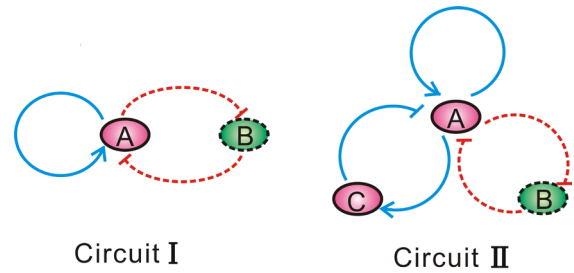
Fig. 1 Schematic of the topological structure of two gene regulatory networks to be studied in this paper: In Circuit Ⅰ, the auto-activation loop (solid line) is the main element of the entire network whereas the toggle switch (dashed line) is the secondary element; In Circuit Ⅱ, the coupled positive and negative feedback loop (solid line) is the main element of the entire network whereas the toggle switch (dashed line) is also the secondary element.

the stable steady states of the bistable system. Owing to the enhancement of the activation threshold, the frequency of the spontaneous switch is independent of input stimulation will decrease. In the activator-repressor circuit, the additional toggle switch can also enhance the stimulation threshold for oscillation and tune the switching frequency without changing the oscillation amplitude even when the input stimulation is kept a constant. The similar dynamical property is also observed in the stochastic oscillator case. These results indicate that the additional toggle switch indeed acts a tinker, providing a specific mechanism of tuning the function of the auto-activation circuit and the activator-repressor circuit, which can be used in the engineering of synthetic circuits.

II. MODELS

Now, we begin by describing our model system using terminologies relevant to gene regulation. Circuit Ⅰ (see figure 1) is a simple two-component regulatory system, which includes two interlinked positive feedback loops. As an activator, protein A binds to and activates its own promoter P_a. As a repressor, component B that is inhibited by protein A inhibits the expression of the A activator by competitively binding to the promoter P_a, forming a double negative feedback loop. Compared to Circuit Ⅰ, Circuit Ⅱ includes another negative feedback loop, where the activator protein A activates the P_c promoter, which further inhibits the A activator by targeting it for degradation. Assume that the kinetics of the regulated activation of the P_a promoter is described by a Hill function with cooperativity n:

$$f(A, k_2, K_{eff}, n) = \frac{k_2 A^n}{A^n + K_{eff}^n} \qquad (1)$$

where A represents the activator concentration in the cell, and the effective activation threshold K_{eff} depends on the

concentration B through the expression $K_{eff}^n = K_1^n + (\gamma B)^m$, In this equation, the k_2 represents the maximum expression rate;

Table 2 Biochemical reactions for circuit Ⅰ and circuit Ⅱ.

Circuit Ⅰ	Circuit Ⅱ	
$P_a \xrightarrow{k\Omega} P_a + mA$	$P_a \xrightarrow{k\Omega} P_a + mA$	$P_c \xrightarrow{k\Omega} P_c + mB$
$P_a \xrightarrow{f(A,B)} P_a + mA$	$P_a \xrightarrow{f(A,B)} P_a + mA$	$P_c \xrightarrow{h(A)\Omega} P_c + mC$
$P_b \xrightarrow{g(A)} P_b + mB$	$P_b \xrightarrow{g(A)} P_b + mB$	$mC \xrightarrow{k_{12}} mC + C$
$mA \xrightarrow{k_4} mA + A$	$mA \xrightarrow{k_4} mA + A$	$mC \xrightarrow{k_{13}} \varnothing$
$mB \xrightarrow{k_5} mB + B$	$mB \xrightarrow{k_5} mB + B$	$C \xrightarrow{k_{14}} \varnothing$
$mA \xrightarrow{k_6} \varnothing$	$mA \xrightarrow{k_6} \varnothing$	$C + A \xrightarrow{k_{15}} C$
$mB \xrightarrow{k_7} \varnothing$	$mB \xrightarrow{k_7} \varnothing$	
$A \xrightarrow{k_8} \varnothing$	$A \xrightarrow{k_8} \varnothing$	
$B \xrightarrow{k_9} \varnothing$	$B \xrightarrow{k_9} \varnothing$	
$f(A,B) = \dfrac{k_2 A^n}{A^n + K_{eff}^n} \quad g(A) = \dfrac{k_3 K_2^m}{K_2^m + A^m} \quad h(A) = \dfrac{k_{11} A^p}{K_3^p + A^p}$		

γ accounts for the strength of competitive inhibition exerted by B; K_1 is the activation threshold of A.

A set of reactions corresponding respectively to Circuit Ⅰ and Circuit Ⅱ are listed in Table 2, where the reaction rates for transcription are assumed to be proportional to a factor Ω, which represents the size of the cell and is taken as a global scaling factor. In the following Gillespie simulation, we set $\Omega = 0.01$. The values of the reaction rates used in simulation are given in Table 3. All the parameter values are set within reasonable biological ranges for a gene regulatory process [27, 28, 26].

Table 3 Parameter values used in our numerical simulation.

	Parameter value			Parameter value	
	Circuit Ⅰ	Circuit Ⅱ		Circuit Ⅰ	Circuit Ⅱ
k_1	0.05nM/(s·molec)	0.0022/(s·molec)	k_9	0.0001 s^{-1}	0.0001 s^{-1}
k_2	1.875nM/(s·molec)	1.875nM/(s·molec)	K_2	5000nM	1000nM
k_3	0.625nM/(s·molec)	0.625nM/(s·molec)	γ	1	0.1
k_4	0.4 s^{-1}	0.4 s^{-1}	p	——	5
k_5	0.4 s^{-1}	0.4 s^{-1}	k_{10}	——	$6.25 \cdot 10^{-2}$ nM/(s·molec)
K_1	5000nM	5000nM	k_{11}	——	0.625nM/(s·molec)
n	2	2	k_{12}	——	0.4 s^{-1}
m	2	2	k_{13}	——	0.1 s^{-1}
k_6	0.1 s^{-1}	0.1 s^{-1}	k_{14}	——	0.0001 s^{-1}
k_7	0.1 s^{-1}	0.1 s^{-1}	k_{14}	——	$4 \cdot 10^{-8}$ /(s·molec)
k_8	0.0001 s^{-1}	0.0001 s^{-1}	K_3	——	3000nM

Assuming that the dynamics of mRNA molecules are much faster than those of proteins with a reason that, usually, the mRNA lifetime is usually in the time range of minutes whereas the protein lifetime is in the range of hours (supposing no enzymatic degradation), we can adiabatically eliminate the equation for mRNA for both circuits, thus leading to the following two-dimensional and three-dimensional equations, respectively

Circuit Ⅰ:

$$\frac{dA}{dt} = \alpha_1 + \beta_1 \frac{A^n}{A^n + K_{eff}^n} - \lambda_1 A$$

$$\frac{dB}{dt} = \beta_2 \frac{K_2^m}{A^m + K_2^m} - \lambda_2 B \tag{2}$$

Circuit Ⅱ:

$$\frac{dA}{dt} = \alpha_1 + \beta_1 \frac{A^n}{A^n + K_{eff}^n} - \delta A C - \lambda_1 A$$

$$\frac{dB}{dt} = \beta_2 \frac{K_2^m}{A^m + K_2^m} - \lambda_2 B \tag{3}$$

$$\frac{dC}{dt} = \alpha_2 + \beta_3 \frac{A^p}{A^p + K_3^p} - \lambda_3 C$$

Where $K_{eff}^n = K_1^n + (\gamma B)^n$,

$\alpha_1 = k_1 k_4 / k_6, \beta_1 = k_2 k_4 / k_6, \lambda_1 = k_8, \beta_2 = k_3 k_5 / k_6, \lambda_2 = k_9$

$\alpha_2 = k_{10} k_{12} / k_{13}, \beta_3 = k_{11} k_{12} / k_6, \lambda_3 = k_{14}, \delta = k_{15}$.

Each composite parameter in (2) and (3) can be calculated from the reaction rates listed in Table 2. Throughout the paper except for a place (see the following), we will fix these parameter values. In addition, we will let the parameter α_1 describe external environment changes (i.e., α_1 represents stimulus).

We aim to show how the additional toggle switch affects the dynamical behavior of both core circuits and their ability in information processing, and summarize some general laws.

III.　Results

A.　Circuits Ⅰ

By analysis, we find that the additional toggle switch has the following effects on the function of the auto-activation circuit.

Enhance the stimulation threshold without significantly altering stable states

Bistability, i.e., the capacity to achieve two alternative states in response to different stimuli, exists ubiquitously in cellular systems. Bistability has fundamental biological significance, notably in cell differential [29], cell fate decision [30], regulation of cell cycle [31], etc. It has increasingly become clear that two or multiple states can be generated from the interactions among the components in a regulatory network. It has been shown that the auto-activation circuit is the simplest circuit to achieve bistability under certain conditions [7]. However, such a circuit is often found to be interlinked with a toggle switch [9]. Therefore, it

is intriguing to investigate the role of the additional toggle switch.

It has been known that each bistable switch establish precise stimulation threshold responding to environmental stimulation. When the stimulation is below the stimulation threshold, the system will stay in the low stable state. And once the stimulation is beyond the threshold, the system will transit from low stable state to high stable state. In one-dimension bifurcation diagram, the stimulation threshold is related to the saddle node bifurcation point (SN). Fig. 2 shows the bifurcation diagram for Circuit I as a function of the stimulation α_1. The solid line represents the stable state, and the dashed line represents the unstable state. The intersection point of the dashed line and the solid line is the saddle node bifurcation point. When α_1 is below the SN point, the system possess two stable states and one unstable state, thus the system display bistability. But when α_1 is beyond the SN point, the system possess only one high stable states and display monostable behavior. If the system is first initiated at the low stable state, the system will stay in the low stable state until the stimulation α_1 transcends the SN point. Once the stimulation is beyond the SN point, the system will transit to the high stable state. Thus we also call SN point as stimulation threshold in the following.

From Fig. 2, we find that the stimulation threshold can be enhanced significantly by adding a toggle switch to the auto-activator circuit. When $\gamma = 0$ (line d in Fig. 2), Circuit I is equivalent to the auto-activation circuit. In this case, we find that the stimulation threshold (SN point) is very small, indicating that small stimulation is sufficient to switch the bistable system from the low stable state to high stable state. When $\gamma = 1$ (line a, b, c in Fig. 2), the toggle switch is added to the auto-activation circuit. We find that the stimulation threshold is enhanced significantly, implying that large stimulation is required to switch the bistable system from low state to high state. In addition, Fig. 2 shows that increasing the maximum expression rate β_2 of B can further tune the stimulation threshold. Actually the stimulation threshold can also be tuned by varying other parameter associated with the toggle switch such as k_1, λ_1 and so on (data is not shown). Therefore, if multiple stimuli regulate the expression rate of component B, cell can tune the stimulation threshold appropriate to their environment. For a fixed $\alpha_1 = 0.1$ (Fig. 2), the system always display bistability when β_2 is larger than 4.5 (line a, b, c in Fig. 2). With the increasing of β_2 from 4.5 to 6.5, we find that two stable states almost keep constant, but the intermediate unstable state varies significantly. If we fix α_1 at other value, we also obtain the same conclusion. Therefore, the additional toggle switch has a little influence on the level of two stable states.
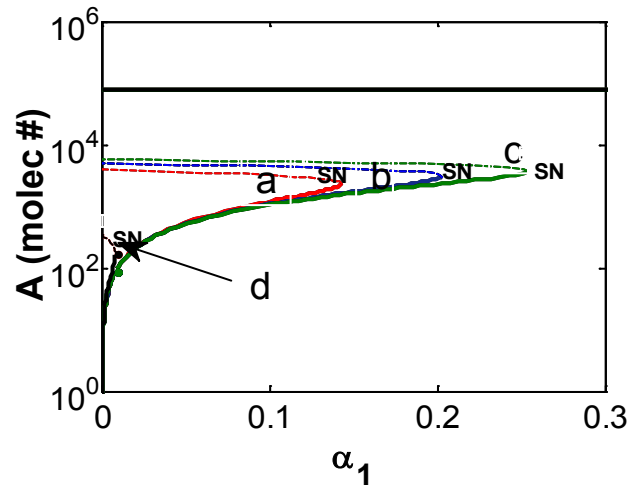

Fig. 2 (color online) Bifurcation diagram with respect to parameter α_1 for Circuit I: The solid lines represent the stable state, and the dashed lines represent the unstable state. The intersection point of dashed line and solid line is the saddle point (SN). Line d corresponds to $\gamma = 0$. Lines a, b, c correspond to $\gamma = 1$ with different $\beta_2 = 2.5, 4.5, 6.5$. The values of other parameters are the same as those listed in Table 3.

We then subject the system to continuous stimulation α_1. The systems are first initiated at low stable state. Fig. 3(A-D) plots the stable steady state of component A as a function of stimulation α_1. The response curve display ultra-sensitivity to the stimulation α_1. Since the system transit from the low stable state to the high stable state rapidly in the ultra-sensitivity regime (Fig. 3(A)), we can also define the ultra-sensitivity regime as stimulation threshold. Fig. 3(A) shows the response curve of the system with different β_2. For each β_2, the system possesses a well defined stimulation threshold. As shown in the figure, increasing β_2 will enhance the stimulation threshold significantly, which is consistent with the conclusion derived from bifurcation analysis. Fig. 3 (B) shows the response curve of the system with different K_2. From Fig. 3 (B), we obtain similar conclusion, e.g. increasing K_2 enhance the stimulation threshold. Actually, other parameters associated with the toggle switch can also tune the stimulation threshold (data is not shown). We also note that the stimulation threshold can be tuned by varying the parameter associated with the auto-activation circuit such as β_1 and λ_1, which are shown in Fig. 3(C) and (D). Comparing Fig. 3(A)(B) with Fig. 3(C)(D) we find that varying the parameter associated with toggle switch has a little influence on the stable steady state of the bistable system. However, varying the parameter associated with the auto-activation circuit can affect the low stable state or high stable state significantly. For example, decreasing β_1 will decrease the high stable state (Fig. 3(C)), and increasing λ_1 will decrease the level of high stable state and low stable state simultaneously (Fig. 3(D)).
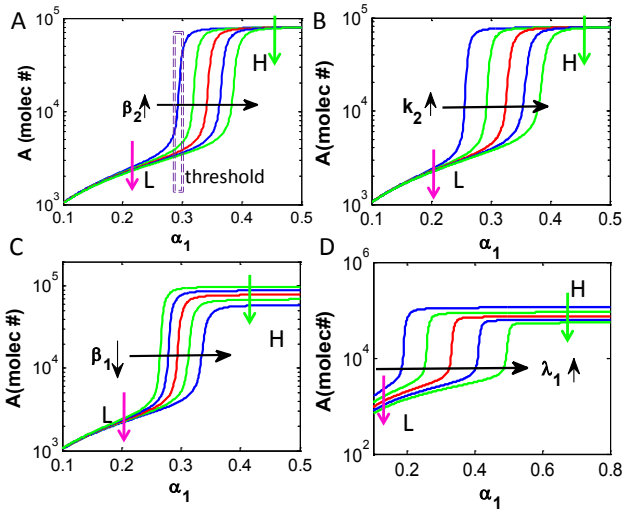
Fig. 3 (color online) The dependence of stimulation threshold on partial parameters of Circuit I, showing that the beginning position for ultrasensitivity, which is defined as stimulation threshold, changes with the parameters. L and H in the figure represent the low stable state and high stable state. Vertical arrows represent monotonic increase or decrease of the stable state whereas horizontal arrows represent the direction of changing parameters. (A) and (B) the response curves when the parameters associated with the toggle switch change. (C) and (D) the response curves when the parameters associated with the auto-activator circuit.

To analytically show that the additional toggle switch can enhance the stimulation threshold regardless of the parameter sets, we analyze the qualitative dependence of the activation threshold on the parameters associated with the toggle switch (note: an exact solution is not easily obtained mainly due to cooperatives n). For simplicity, here we consider component B as external stimulation which can be tuned artificially. Then the stimulation threshold α_c should satisfy the following two equations:

$$F(A_c, \alpha_c) = \alpha_c + \beta_1 \frac{A_c^n}{A_c^n + K_1^n + (\gamma B)^n} - \lambda_1 A_c = 0 \quad (4)$$

$$\frac{\partial F}{\partial A_c}(A_c, \alpha_c) = 0 \quad (5)$$

where A_c is the steady state of component A corresponding to stimulation α_c. Since the basal expression rate is often very low, we assume that $\alpha_1 \ll 1$. Then The combination of Eqns. (4) and (5) yields

$$\alpha_c = \lambda_1 \sqrt[n]{(n-1)(K_1^n + (\gamma B)^n)} - \beta_1 \frac{n-1}{2n-1} \quad (6)$$

Since in the steady state $B = \frac{\beta_2}{\lambda_2} \frac{K_2^m}{A_c^m + K_2^m}$, increasing β_2 and K_2 will enhance the steady state of B, which further enhance the activation threshold α_c. Such a simple analysis indicates that the toggle switch can enhance the activation threshold independent on the parameters.

To analytically show that the steady states are insensitivity to the additional toggle switch, we apply sensitivity analysis for the system. Here, we also view the component B as external stimulation and kept it as a constant. Then the steady states (A_s, B_s) (A_s is the concentration of A

and B_s is the concentration of B) should satisfy the following equation:

$$F(A_s, B_s) = \alpha_1 + \beta_1 \frac{A_s^n}{A_s^n + K_1^n + (\gamma B_s)^n} - \lambda_1 A_s = 0 \quad (7)$$

The absolute sensitivity to the component B can be calculated by:

$$\frac{\partial A_s}{\partial B_s} = -\frac{\partial F / \partial B_s}{\partial F / \partial A_s} \approx \frac{n\gamma^n B_s^{n-1} A_s}{(n-1)(K_1^n + \gamma^n B_s^n) - A_s^n} \quad (8)$$

Note that for the low steady state, $A_s \ll K_1, B_s \gg K_1$, thus

$$\frac{\partial A_s}{\partial B_s} \approx \frac{nA_s}{(n-1)B_s} \ll 1; \quad (9)$$

For the high steady state, $A_s \gg K_1, B_s \ll K_1$, thus

$$\left| \frac{\partial A_s}{\partial B_s} \right| \approx \left| \frac{n\gamma^n B^{n-1} A_s}{-A_s^n} \right| = \frac{n\gamma^n B_s^{n-1}}{A_s^{n-1}} \ll 1. \quad (10)$$

In both case, the steady state A_s is insensitivity to the concentration of component B. The relative sensitivity to all the parameters in the full system is difficult to be solved analytically, but we can approximate the relative sensitivity using the following numerical method[32]:

$$\frac{p dA_s}{A_s dp} \approx \frac{[A_s(p + \Delta p) - A_s(p)] / A_s(p)}{\Delta p / p} \quad (11)$$

Where p is the parameter of the system, here we chose $\Delta p / p = 0.1$. Fig.4 (A) shows the relative sensitivity of high steady state and low steady state to all parameters. We find that the former is sensitive to two parameters β_1 and λ_1 whereas the latter is sensitive to two parameters α_1 and λ_1. Moreover, both are robust to the parameters associated with the additional toggle switch (i.e. β_2, K_2, λ_2). This is in accord with our theoretical prediction. To verify the generality of the above result, we also perform the global robustness to analysis the sensitivity of the system [33]. First, 1000 parameter vectors $p = (p_1, p_2 ... p_8)$ are sampled from the whole parameter space. The range of each component is $[0.9p_i^0, 1.1p_i^0]$, where the p_i^0 is the nominal value listed in Table 2. Then, for each sampled parameter vector p we compute the relative variation of steady state:

$$\Delta S = \left| [A_s(p) - A_s(p^0)] / A_s(p^0) \right| \quad (12)$$

If $\max(\Delta s_l, \Delta s_h) < 5\%$ (where Δs_l and Δs_h represent the relative variation for the high and the low steady state respectively), then we accept the corresponding parameter vector and view that the corresponding steady state is robust against the parameters perturbation after a global simulation, thus obtaining a viable parameter sets. Next, we perform the principle component analysis (PCA), which is a useful tool to analyze sensitivity for high dimension systems. Fig. 4(B) shows standard variation along each PCA axis[34]. We observe that the variation along the last two PCA axes is significantly small in contrast to the other PCA axes, indicating that the system is most sensitive in the directions along the last two component axes. Note that each PCA axis can be represented as the linear combination of the parameters. We observe that the combination of parameters
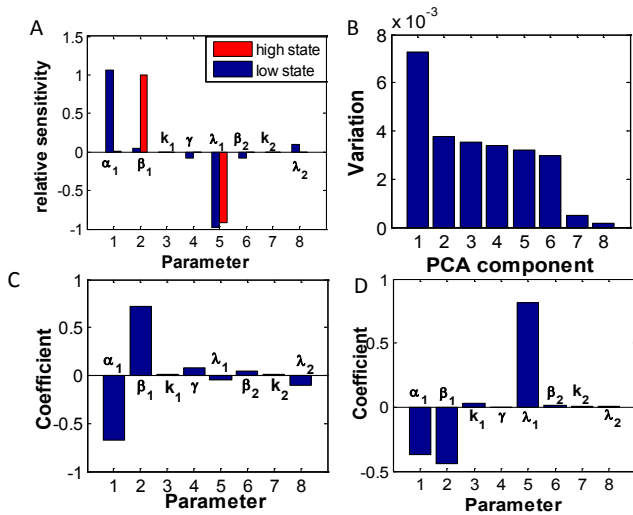
Fig. 4 (color online) Result by sensitivity analysis for circuit Ⅰ. (A) shows the relative local sensitivity of the stable steady states of the bistable system. (B) shows the standard variation along each principal component. (C) and (D) show the linear combination of last two principle component axes that can be represented as the linear combination of parameters in PCA analysis.

α_1, β_1 and γ_1 dominates the last two PCA axes (Fig. 4 (C) and (D)), implying that the steady states of the system are most sensitive to these parameters and insensitive to the parameters associated with the toggle switch. Combining the above local relative sensitivity analysis and global sensitivity analysis, we conclude that the steady states are insensitive to the toggle switch for all parameters associated with the core circuit.

Enhancing the response time and mean first passage time (mFPT)

Response time is another important temporal property for the bistable system, and is defined as the time taken for the system to switch from the low stable state to the high stable state. For a biological system, the response time may vary in a wide range. For example, in systems associated with brain injury a short stimulus gives rise to an immediate response [35]. But during the maturation of *oocytes*, progesterone stimulation caused a delayed response [30]. To measure the response time, we assume that the bistable system is initially settled in the low stable state and subjected to the step signal. Fig. 5(A) shows the response of the circuit A to the step signal. The step signal is first initiated at $\alpha_1 = 0.01$ and rapidly transit to $\alpha_1 = 0.11$ at the moment $t = 4000$. From this subfigure, we observe that varying parameter β_2 can tune the response time significantly. Thus, we further define the response time as the time required to reach the midpoint between the low stable state and high stable state after a signal transition occurs. Fig. 5(B) shows the response time as a function of β_2. Increasing the value of β_2 enhances the response time of the bistable switch, implying that more time is taken as that for the system to reach the high steady state. Note that the response time increases rapidly and tends finally to infinite when β_2

approach a critical value β_c, indicating that the system cannot transit to the high stable state when β_2 is beyond β_c.

In the stochastic condition, even though there is no external stimulus, the intrinsic noise can drive the system beyond the stimulation threshold and induce spontaneous switch from low stable state to the high stable state. To capture the effect of these fluctuations, we employ the Gillespie's first reaction method [36] to simulate the chemical reactions listed in table 1. Fig. 5(C) shows examples of stochastic simulation with an initial activator number of 200 molecules per cell. Red curves demonstrate the time course of A activation for system with maximum transcription rate of B $k_3 = 0.225$ and blue curves for system with $k_3 = 0.425$. Comparing red curves with blue curves, we find that increasing the transcription rate k_3 mainly leads to different time delay of the transition from low stable state to high stable state, while the level of the low activated state and high activated state for these two cases are almost kept constant.
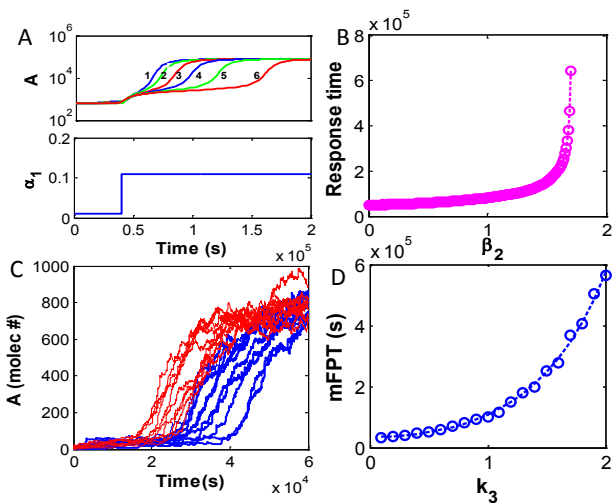
Fig. 5 (color online) Response time and mean first passage time. (A) Response of component A to step signal, where the dashed represent the step signal initiated at $\alpha_1 = 0.01$ and rapidly transits to $\alpha_1 = 0.11$ at time $t = 4000$. From left to right, β_2 is 0.5, 0.6, 0.7, 0.8, 0.9 and 1.0. (B) The response time of bistable system subjected to step signal. Increasing the value of β_2 will enhance the response time. (C) Time series of stochastic switch in bistable system for $k_3 = 0.225$ (red line) and blue curves when $k_3 = 0.425$ (Blue line). (D) The mean first passage time of the noise induced switch for $K_2 = 5000$, the value of other parameters are same as those in Table 2.

An important index to measure the switch frequency is the mean first passage time (mFPT)[37, 38] (i.e. the average time it takes to switch gene expression states from low stable state to high stable state). The mFPT is inversely related to the number of cells in a bacterial population that transit to the high stable state during a limited time window. In Fig. 5(D), we present the mFPT versus the value of the maximal transcription rate k_3 for $K_2 = 5000$. It can be seen that the MFPT increase exponentially as the increasing of k_3. The

mFPT for the system increase more than 17 times when k_3 increase from 0.1 to 1.4.

B. Circuit Ⅱ

By analysis, we find that the additional toggle switch has the following effects on the function of the activator-repressor circuit.

Enhance the stimulation threshold for oscillation

Previous studies have shown that the activator-repressor circuit can exhibit various dynamical behaviors including excitability and oscillation. Biological oscillations underlie many physiological functions in cells, ranging from basic processes such as cell growth and division [31] to evolutionary environmental adaptation such as circadian rhythmicity [39]. Many circuit architectures have been proposed to explain the observed periodic behavior in terms of limit-cycle attractors of nonlinear dynamical models [3]. The activator-repressor circuit is one of the regulatory networks used to investigate relaxation-type oscillations.

Mathematically, this oscillation behavior arises from Hopf bifurcation or SNIC bifurcation[27]. In this paper we only focus on the oscillation arises from SNIC bifurcation. Fig. 6 shows a bifurcation diagram, where thick lines represents the limit cycle, and thin solid lines and dashed lines represent the stable state and unstable fixed points, respectively. When the stimulation α_1 is beyond the SNIC bifurcation point (at which point the saddle point collides with a stable limit cycle that surrounds the unstable spiral point), the system display oscillation. But when stimulation α_1 is below the SNIC point, the system will stay in the low stable state. Fig. 6 also shows the bifurcation diagram when we vary the maximum transcription rate β_2 of B. Increasing β_2 has a little influence on the shape of the limit cycle, but altering the position of the SNIC bifurcation point remarkably. Intuitively, when the stimulation is low, the auto-positive feedback loop cannot be activated and the system stays in the low stable state. Large stimulation can activate the auto-positive feedback loop and further increase the concentration of A. If the concentration of A reaches a critical value, the negative feedback is activated which drive the system back to the low state. Increasing β_2 can enhance the activation threshold K_{eff}, which make the auto-positive feedback difficult to be activated. Since when concentration of A is low, the auto- positive feedback loop is not activated, increasing β_2 will not affect the concentration of A. When concentration of A is high, the concentration of B is very low. Therefore the effect of increasing β_2 is negligible. Since the SNIC act as the same role as stimulation threshold for oscillation, our results suggest that the additional toggle switch in the activator-repressor circuits enhance the stimulation threshold to generate oscillation.
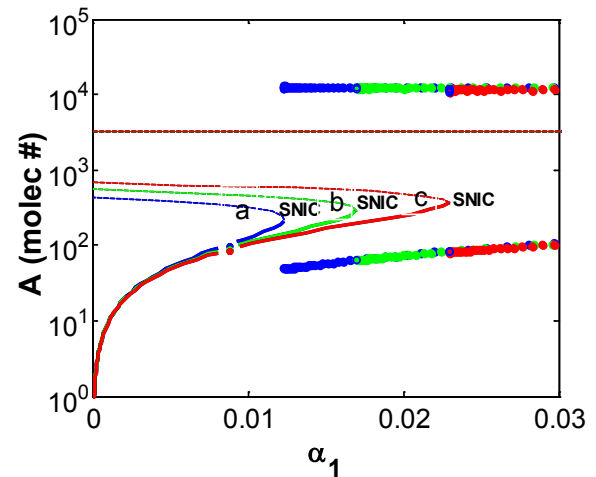

Fig. 6(color online) Bifurcation diagram for Circuit B. The thick lines represent the limit cycle, and the solid lines and dashed lines represent the stable state and unstable fixed points, respectively. The saddle point collides with a stable limit cycle at the SNIC point. Line a, b and c represent bifurcation diagram for $\beta_2 = 2.5, 4.5$ and 6.5, the value of other parameters are same as those in Table 2.

Increase oscillation period without affecting oscillation amplitude

It has been known that the single negative feedback loop with significant non-linearity or time delay can generate oscillation. While the positive feedback loops are not essential to generate oscillation. Theoretic comparison of negative-feedback -only and negative-plus-positive models leads to the conclusion that the positive feedback loop significantly increases the frequency range of oscillator without significantly altering the amplitude[10]. However, it is still unclear that which kind of positive feedback loop is more appropriate to achieve tunable frequency. Furthermore, in the previous studies, the frequency can only be tuned by changing the input stimulus. In this subsection, we will show that the additional toggle switch can tune the frequency independent of the input stimulus, which provide a new mechanism to achieve tunable frequency with nearly constant amplitude.

Fig. 7(A) shows the shape of oscillation when we vary the maximum expression rate β_2 of B from 4.5 to 5.0, but keep the stimulus $\alpha_1 = 0.03$. It can be seen that increasing the value of β_2 will increase the period of the oscillation but do not significantly altering the amplitude of the oscillation. Fig. 7(B) shows the normalized frequency and amplitude when we increase β_2 from 4.5 to 5.6. The frequency decrease about 25 fold but the amplitude almost maintains the same. As β_2 approaches 5.6, we observe that the frequency decreases rapidly. This would be because when the system approaches the SNIC point from the right side (referring to Fig. 6), the frequency tends to 0.
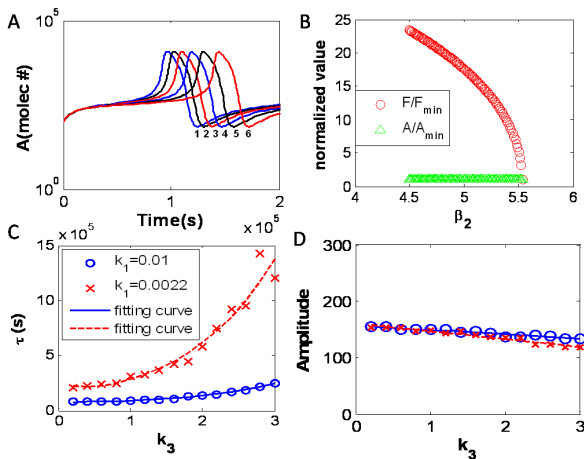
Fig. 7(color online) Frequency tunability by the toggle switch (A) The shape of the limit cycle when the value of β_2 is 4.5, 4.6, 4.7, 4.8, 4.9 and 5 (from left to right), the value of other parameters are same as those in Table 2. (B) The normalized amplitude and frequency as a function of β_2, where F and A denote frequency and amplitude of the limit cycle respectively, F_{min} and A_{min} denote the frequency and amplitude for $\beta_2 = 5.6$. (C) and (D) the mean switch time and the amplitude of oscillation in stochastic condition for $k_1 = 0.01$ ($\bigcirc$) and $k_1 = 0.0022$ ($\times$), the value of other parameters are same as those in Table 2.

In the stochastic condition, we use Gillespie's first reaction method [36] to simulate the chemical reactions listed in table 1. We use the mean switching time (namely, the average time between spontaneous switching events) to quantify the frequency of oscillation. In Fig. 7 (C) and (D), we present the mean switching time τ versus the transcription rate k_3 of component B . When $k_1 = 0.01$ (the basal transcription rate of component A), the system display oscillation in both deterministic condition (data is not shown) and stochastic condition. Increasing the transcription rate k_3 from 0.2 to 3 will enhance the mean switch time from 7869 s to 25010 s, while the amplitude of oscillation decrease from 157 to 133. The frequency of oscillation change more drastically than the amplitude of oscillation. When $k_1 = 0.0022$, the system cannot display oscillation in deterministic condition (data is not shown), but displays stochastic oscillations in the stochastic case. We also call this phenomenon as stochastic oscillator. Moreover, we find that the frequency of stochastic oscillations increases more drastically when the transcription rate k_3 increases from 0.2 to 3.

IV. CONCLUSION AND DISCUSSION

The toggle switch is found in various genetic networks across all organisms. It has been shown that the toggle switch can serve as a basic circuit to achieve bistability and hysteresis [40]. However, in many cases, the toggle switch is not essential but is secondary to a functional network [14, 15]. For two simplest circuits, the auto-activator and activator-repressor circuits, which generate two different kinds of dynamical behaviors, bistability and oscillation, we have shown that the toggle switch acts as a tinker to both circuits, that is, it can tune or elaborate the function of both circuits.

Bistability is a fundamental behavior of biological systems and has been studied extensively through experiments, theoretical analysis and numerical simulation [41, 42, 7, 43, 9]. The auto-activator is the simplest circuit to achieve the bistable switch [6, 44]. We have shown that when the toggle switch is added to the auto-activator circuit, it can elaborate the function. Specifically, the toggle switch can enhance the stimulation threshold for bistable switch but does not significantly alter the two stable states of this circuit. Moreover, it can tune the frequency of random switch resulted from molecular noise. These results would be of biological significance. In fact, recall that in the competence development of *Bacillus subtilis* [45, 11, 12], the auto-activator comprised of ComK is the core architecture to generate a bistable expression pattern. Previous experiments showed that the toggle switch comprised of RoK and ComK [45] can affect the proportion of competence cells. Our result can provide an explanation for this phenomenon since we have shown that the toggle switch can enhance the stimulation threshold for bistable switch but the enhanced stimulation threshold can decrease switching frequency.

Oscillations also occur in many contexts such as metabolism, signaling, and development. The lest requirement for a circuit to generate oscillations is a negative feedback loop with time delay [3], but the corresponding oscillations are relatively unstable. The activator-repressor system is one of the most common architectures to achieve robust oscillations [46]. We have shown that the additional toggle switch can enhance the stimulation threshold for this circuit to generate oscillations. In addition, it can tune the frequency of oscillations without significantly altering the amplitude of oscillations. In contrast to a previous study, which showed that positive feedback loop can tune frequency to a wide range but keep a near constant amplitude [10], our study suggests that the additional toggle switch can provide another mechanism for achieving a tunable frequency with a near constant amplitude.

Except for bistability and oscillation, excitability is an interesting behavior, and can occur in a regulatory network with interlinked positive and negative feedback loops [12, 26], exemplified by a transient differential into competence in *Bacillus subtilis* [12]. We have numerically found that the additional toggle switch can also modify the excitable behavior (data are not shown). As shown in Fig. 6, when α_1 is below the SNIC bifurcation point, the system possesses one low stable state, one saddle node, and one unstable spiral state, imply that it can display excitability. Only stimulation that transcends the SNIC point can trigger a large excitable response and then return to the low stable state. So when SNIC is enhanced, a large perturbation is required to trigger an excitable response. We can show that the additional toggle switch tunes the activation threshold for excitability. In addition, it does not significantly alter the amplitude of oscillations, nor can it affect the high state in excitable switch.

Besides two simple architectures discussed here, the toggle switch is found as a secondary module in more complex networks. The insight gained from the study of the simple motifs would provide a basis for understanding more complex networks assembled by simple building blocks. A clearer understanding for the role of toggle switch as a tinker

would be important for bio-engineering or artificial control of specified components, interaction, and even network functions. It is expecting that the results presented here provide a new view on how gene expression is regulated as well as guidelines for experiments.

REFERENCES

[1]. Kim, D.,Kwon, Y.K. and Cho, K.H., "Coupled positive and negative feedback circuits form an essential building block of cellular signaling pathways", BioEssays, 2007, 29, (1), pp. 85-90.

[2]. Ma, W.,Trusina, A.,El-Samad, H.,Lim, W.A. and Tang, C., "Defining network topologies that can achieve biochemical adaptation", Cell, 2009, 138, (4), pp. 760-773.

[3]. Novak, B. and Tyson, J.J., "Design principles of biochemical oscillators", Nature Reviews Molecular Cell Biology, 2008, 9, (12), pp. 981-991.

[4]. Tyson, J.J. and Novok, B., "Functional motifs in biochemical reaction networks", Annual review of physical chemistry, 2010, 61, pp. 219-240.

[5]. Brandman, O.,Ferrell Jr, J.E.,Li, R. and Meyer, T., "Interlinked fast and slow positive feedback loops drive reliable cell decisions", Science's STKE, 2005, 310, (5747), pp. 496.

[6]. Brandman, O. and Meyer, T., "Feedback loops shape cellular signals in space and time", Science's STKE, 2008, 322, (5900), pp. 390.

[7]. Ferrell, J.E., "Feedback regulation of opposing enzymes generates robust, all-or-none bistable responses", Current Biology, 2008, 18, (6), pp. R244-R245.

[8]. Nguyen, L.K., "Regulation of oscillation dynamics in biochemical systems with dual negative feedback loops", Journal of The Royal Society Interface, 2012, pp.

[9]. Saini, S.,Ellermeier, J.R.,Slauch, J.M. and Rao, C.V., "The role of coupled positive feedback in the expression of the SPI1 type three secretion system in Salmonella", PLoS pathogens, 2010, 6, (7), pp. e1001025.

[10]. Tsai, T.Y.C.,Choi, Y.S.,Ma, W.,Pomerening, J.R.,Tang, C. and Ferrell Jr, J.E., "Robust, tunable biological oscillations from interlinked positive and negative feedback loops", Science's STKE, 2008, 321, (5885), pp. 126.

[11]. Smits, W.K.,Eschevins, C.C.,Susanna, K.A.,Bron, S.,Kuipers, O.P. and Hamoen, L.W., "Stripping Bacillus: ComK auto-timulation is responsible for the bistable response in competence development", Molecular microbiology, 2005, 56, (3), pp. 604-614

[12]. Süel, G.M.,Garcia-Ojalvo, J.,Liberman, L.M. and Elowitz, M.B., "An excitable gene regulatory circuit induces transient cellular differentiation", Nature, 2006, 440, (7083), pp. 545-550.

[13]. Suel, G.M.,Kulkarni, R.P.,Dworkin, J.,Garcia-Ojalvo, J. and Elowitz, M.B., "Tunability and noise dependence in differentiation dynamics", Science's STKE, 2007, 315, (5819), pp. 1716.

[14]. Hoa, T.T.,Tortosa, P.,Albano, M. and Dubnau, D., "Rok (YkuW) regulates genetic competence in Bacillus subtilis by directly repressing comK", Molecular microbiology, 2002, 43, (1), pp. 15-26.

[15]. Ferrell Jr, J.E.,Tsai, T.Y.C. and Yang, Q., "Modeling the cell cycle: why do certain circuits oscillate?" Cell, 2011, 144, (6), pp. 874-885.

[16]. Pomerening, J.R.,Kim, S.Y. and Ferrell, J.E., "Systems-level dissection of the cell-cycle oscillator: bypassing positive feedback produces damped oscillations", Cell, 2005, 122, (4), pp. 565-578.

[17]. Cherry, J.L. and Adler, F.R., "How to make a biological switch", Journal of Theoretical Biology, 2000, 203, (2), pp. 117-133.

[18]. Gardner, T.S.,Cantor, C.R. and Collins, J.J., "Construction of a genetic toggle switch inEscherichia coli", Nature, 2000, 403, pp. 339-342.

[19]. Reynolds, A.R.,Tischer, C.,Verveer, P.J.,Rocks, O. and Bastiaens, P.I.H., "EGFR activation coupled to inhibition of tyrosine phosphatases causes lateral signal propagation", Nature cell biology, 2003, 5, (5), pp. 447-453.

[20]. Yates, A.,Callard, R. and Stark, J., "Combining cytokine signalling with T-bet and GATA-3 regulation in Th1 and Th2 differentiation: a model for cellular decision-making", Journal of theoretical biology, 2004, 231, (2), pp. 181-196.

[21]. Loinger, A. and Biham, O., "Analysis of genetic toggle switch systems encoded on plasmids", Physical review letters, 2009, 103, (6), pp. 68104.

[22]. Zhou, T.,Zhang, J.,Yuan, Z. and Chen, L., "Synchronization of genetic oscillators", Chaos: An Interdisciplinary Journal of Nonlinear Science, 2008, 18, (3), pp. 037126-037126-20.

[23]. Krishna, S.,Semsey, S. and Jensen, M.H., "Frustrated bistability as a means to engineer oscillations in biological systems", Physical Biology, 2009, 6, pp. 036009.

[24]. Oikonomou, C. and Cross, F.R., "Frequency control of cell cycle oscillators", Current opinion in genetics & development, 2011, 20, (6), pp. 605-612.

[25]. Lee, J.H. and Sancar, A., "Regulation of apoptosis by the circadian clock through NF-kB signaling", Proceedings of the National Academy of Sciences, 2011, 108, (29), pp. 12036.

[26]. Turcotte, M.,Garcia-Ojalvo, J. and Suel, G.M., "A genetic timer through noise-induced stabilization of an unstable state", Proceedings of the National Academy of Sciences, 2008, 105, (41), pp. 15732.

[27]. Rue, P. and Garcia-Ojalvo, J., "Gene circuit designs for noisy excitable dynamics", Mathematical Biosciences, 2011, pp.

[28]. Rue, P.,Suel, G.M. and Garcia-Ojalvo, J., "Optimizing periodicity and polymodality in noise-induced genetic oscillators", Physical Review E, 2011, 83, (6), pp. 061904.

[29]. Becskei, A.,Seraphin, B. and Serrano, L., "Positive feedback in eukaryotic gene networks: cell differentiation by graded to binary response conversion", The EMBO journal, 2001, 20, (10), pp. 2528-2535.

[30]. Xiong, W. and Ferrell, J.E., "A positive-feedback-based bistable 'memory module' that governs a cell fate decision", Nature, 2003, 426, (6965), pp. 460-465.

[31]. Pomerening, J.R.,Sontag, E.D. and Ferrell, J.E., "Building a cell cycle oscillator: hysteresis and bistability in the activation of Cdc2", Nature Cell Biology, 2003, 5, (4), pp. 346-351.

[32]. Zi, Z., "Sensitivity analysis approaches applied to systems biology models", Systems Biology, IET, 2011, 5, (6), pp. 336-346.

[33]. Hafner, M.,Koeppl, H.,Hasler, M. and Wagner, A., "Gllocal robustness analysis and model discrimination for circadian oscillators", PLoS computational biology, 2009, 5, (10), pp. e1000534.

[34]. Barnes, C.P.,Silk, D.,Sheng, X. and Stumpf, M.P.H., "Bayesian design of synthetic biological systems", Proceedings of the National Academy of Sciences, 2011, 108, (37), pp. 15190-15195.

[35]. Bordet, R.,Deplanque, D.,Maboudou, P.,Puisieux, F.,Pu, Q.,Robin, E.,Martin, A.,Bastide, M.,Leys, D. and Lhermitte, M., "Increase in endogenous brain superoxide dismutase as a potential mechanism of lipopolysaccharide-induced brain ischemic tolerance", Journal of Cerebral Blood Flow & Metabolism, 2000, 20, (8), pp. 1190-1196.

[36]. Gillespie, D.T., "Exact stochastic simulation of coupled chemical reactions", The journal of physical chemistry, 1977, 81, (25), pp. 2340-2361.

[37]. Kobayashi, T.J., "Connection between Noise-Induced Symmetry Breaking and an Information-Decoding Function for Intracellular Networks", Physical Review Letters, 2011, 106, (22), pp. 228101.

[38]. Mehta, P.,Mukhopadhyay, R. and Wingreen, N.S., "Exponential sensitivity of noise-driven switching in genetic networks", Physical Biology, 2008, 5, pp. 026005.

[39]. Goldbeter, A., "Computational approaches to cellular rhythms", Nature, 2002, 420, (6912), pp. 238-245.

[40]. Ferrell, J.E., "Self-perpetuating states in signal transduction: positive feedback, double-negative feedback and bistability", Current opinion in cell biology, 2002, 14, (2), pp. 140-148.

[41]. Chang, D.-E.,Leung, S.,Atkinson, M.R.,Reifler, A.,Forger, D. and Ninfa, A.J., "Building biological memory by linking positive feedback loops", Proceedings of the National Academy of Sciences, 2010, 107, (1), pp. 175-180.

[42]. Domingo-Sananes, M.R. and Novak, B., "Different effects of redundant feedback loops on a bistable switch", Chaos: An Interdisciplinary Journal of Nonlinear Science, 2010, 20, (4), pp. 045120-045120-11.

[43]. Mitrophanov, A.Y. and Groisman, E.A., "Positive feedback in cellular control systems", Bioessays, 2008, 30, (6), pp. 542-555.

[44]. Liu, Q. and Jia, Y., "Fluctuations-induced switch in the gene transcriptional regulatory system", Physical Review E, 2004, 70, (4), pp. 041907.

[45]. Maamar, H.,Raj, A. and Dubnau, D., "Noise in gene expression determines cell fate in Bacillus subtilis", Science's STKE, 2007, 317, (5837), pp. 526.

[46]. Gerard, C.,Gonze, D. and Goldbeter, A., "Effect of positive feedback loops on the robustness of oscillations in the network of cyclin dependent kinases driving the mammalian cell cycle", FEBS Journal, 2010, pp.